Remnant Geometric Hall Response in a Quantum Quench

Justin H. Wilson,[1,*] Justin C. W. Song,[1,2,†] and Gil Refael[1,2]
[1]Institute of Quantum Information and Matter and Department of Physics, California Institute of Technology, Pasadena, California 91125, USA
[2]Walter Burke Institute of Theoretical Physics, California Institute of Technology, Pasadena, California 91125, USA
(Received 29 March 2016; published 30 November 2016)

Out-of-equilibrium systems can host phenomena that transcend the usual restrictions of equilibrium systems. Here, we unveil how out-of-equilibrium states, prepared via a quantum quench in a two-band system, can exhibit a nonzero Hall-type current—a remnant Hall response—even when the instantaneous Hamiltonian is time reversal symmetric (in contrast to equilibrium Hall currents). Interestingly, the remnant Hall response arises from the coherent dynamics of the wave function that retain a remnant of its quantum geometry postquench, and can be traced to processes beyond linear response. Quenches in two-band Dirac systems are natural venues for realizing remnant Hall currents, which exist when either mirror or time-reversal symmetry are broken (before or after the quench). Its long time persistence, sensitivity to symmetry breaking, and decoherence-type relaxation processes allow it to be used as a sensitive diagnostic of the complex out-of-equilibrium dynamics readily controlled and probed in cold-atomic optical lattice experiments.

DOI: 10.1103/PhysRevLett.117.235302

Subtle quantum coherences encoded in the topology of crystal wave functions are responsible for a wide array of robust quantum phenomena [1–4], e.g., the quantum Hall effect. While originating in the solid state, cold atoms have recently become a system of choice for experimentally unraveling topology on the microscopic level [5–7] due to the array of new probes available. For example, these probes have been used to image the skipping orbits (edge states) in a cold-atomic quantum Hall system [8] and directly measure the Berry curvature [9] and Zak phase [10] in cold-atomic topological bands.

One readily available tool is the quantum quench, which can be used to probe band properties, including topology [11–13]. In quantum quenches, a state, prepared in the many-body ground state of a Hamiltonian $H(\zeta)$, undergoes a sudden change in a physical parameter ζ (e.g., lattice depth, detuning), setting the system into dynamical evolution far from equilibrium [14]. The ease with which distinct Hamiltonians can be accessed via quenches and driving opens up tantalizing possibilities of achieving new out-of-equilibrium phenomena with no equilibrium analog [15–22].

Here, we unveil a completely new type of dynamical response achieved in out-of-equilibrium states (OESs) which can be prepared via quantum quenches. In particular, we show that certain OES can feature a remnant Hall response even when the instantaneous Hamiltonian preserves time-reversal symmetry (TRS). Remnant Hall responses arise due to the geometric evolution of OES postquench. Intriguingly, it possesses features such as a Hall current that saturates to a nonzero value at long times [Fig. 1(e)] that have no equilibrium analog.

This can be most easily illustrated for noninteracting and clean Dirac systems, where many-body states can be represented as a collection of pseudospinors on a Bloch sphere [Fig. 1(b)–1(d)]. In these, a state is prepared in the ground state of a Dirac Hamiltonian $H(\Delta)$, with TRS breaking gap Δ [Fig. 1(a)]. At $t = 0$, the Hamiltonian is quenched to $H(\Delta = 0)$ (where TRS is preserved), yielding dynamics for OES, with the pseudospinors exhibiting Larmor precession [Fig. 1(c)].

To probe OES, a short pulse of strength $\mathbf{A} = \int dt \mathbf{E}(t)$ can be applied to the system at time $t = t_1$ [Figs. 1(a, e)], shifting the Larmor orbits along $\mathbf{E}$. Averaged over one cycle, longitudinal momentum along $\mathbf{E}$ increases. However, in addition to this, the constraint of pseudospinors being on the Bloch sphere allows a transverse shift to accumulate. As a result, at long times $t = t_2$, we obtain a remnant Hall current

$$\mathbf{J}_{\mathrm{Hall}}(t_1, t_2 \to \infty) = \Xi^{\infty}_{\mathrm{Hall}}(t_1)\hat{\mathbf{z}} \times \mathbf{A}, \tag{1}$$

that persists long after the applied pulse $\mathbf{E}(t)$ has passed, as shown in Fig. 1(e). Here, $\Xi^{\infty}_{\mathrm{Hall}}$ is a nonuniversal function depending on t_1 and model specifics described below. Instead of the Hall conductivity, we focus on the total current and $\Xi^{\infty}_{\mathrm{Hall}}$ because (i) time-translational symmetry is broken and (ii) the effect described here is inherently beyond linear response. Additionally, while we use the language of electromagnetic response, in cold-atom optical lattices, $e\mathbf{A}$ can be easily effected by a shift in momentum $\Delta\mathbf{p}$ brought on by a sudden force; in such systems, $\mathbf{J}_{\mathrm{Hall}}$ takes the form of a particle current.

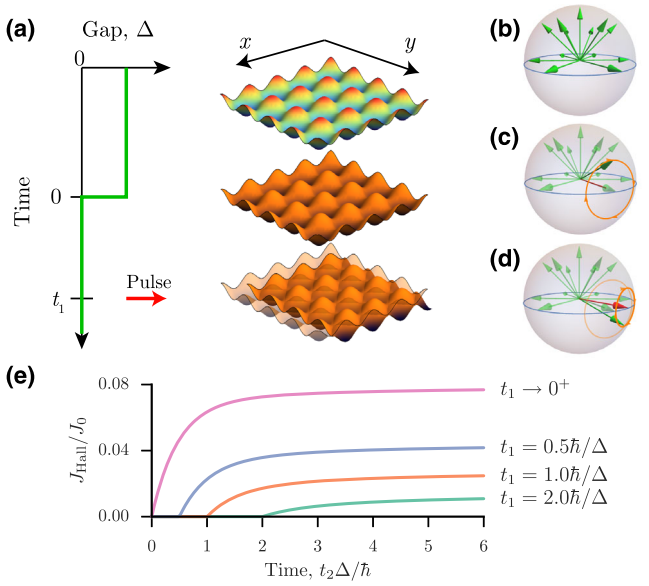

FIG. 1. (a) Quantum quenches implemented in cold-atomic optical lattices where a parameter in the Hamiltonian is changed suddenly shown by change in color of optical lattice. Here, the green curve shows $\Delta(t)$ quench. (b) Pseudospinors on a Bloch sphere prepared in the Chern insulator state of the Haldane model (c) exhibit Larmor precession after the Hamiltonian is quenched into zero gap. (d) The pseudospinors can acquire a transverse shift after the system is pulsed in the longitudinal direction. (e) Remnant Hall response for quenching protocol described in Eq. (3) [and panels (b)–(d)]. Here characteristic $J_0 = (e^2/h)(\Delta^2/e\hbar v_F)$ with pulse strength $A_x = 0.1\,\Delta/ev_F$.

Remnant Hall currents [Eq. (1), Fig. 1(e)] are strikingly different from those found in equilibrium systems in two respects: (1) Without relaxation processes, they persist at infinite times after an applied pulse and (2) involve momentum shifts in the Fermi sea. Therefore, as the Fermi sea relaxes, the Hall current degrades (as would be expected from general considerations [23,24]).

A useful analogy between the coherent evolution of spins in nuclear magnetic resonance (NMR) protocols and our pseudospins can be drawn. In the former, the decay of the NMR signal can be used as a sensitive diagnostic of scattering, for, e.g., spin-spin, spin-environment relaxation. As we argue below, purely dephasing phenomena, e.g. described by T_2, have no effect on the remnant Hall response. However, energy relaxation in the form of T_1 degrades the effect. Therefore, we anticipate that the decay profile of $\mathbf{J}_{\rm Hall}$ that arises from coherent pseudospinor evolution can be used as a diagnostic of relaxation and/or thermalization processes in OES when interactions and disorder are allowed.

The ease with which Dirac-type [9] and other spin-orbit coupled Hamiltonians [5] can be constructed in setups for ultracold bosons and fermions allow these effects to be easily accessed; however, we find that fermions are more readily amenable. In order to observe the Hall effect and separate it from an overwhelming longitudinal response, we propose a time-of-flight setup in the direction perpendicular to the applied pulse while keeping a confining potential in the direction of the applied pulse. In such an experimental setup, the gap, as tuned by Zeeman coupling or "shaking" of the cold atom lattice, is suddenly turned off. The "pulse" is then implemented some time after the quench by applying a sudden and brief force upon the system (e.g., tilting the confining potential for a very short time).

Now, let us explain the effect with a two-band Hamiltonian $H(\Delta) = \sum_{\mathbf{p}} c^\dagger_{\mathbf{p}} h(\mathbf{p},\Delta) c_{\mathbf{p}}$ with $c_{\mathbf{p}} = (c_{+,\mathbf{p}}, c_{-,\mathbf{p}})^T$ and

$$h(\mathbf{p},\Delta) = \epsilon_0(\mathbf{p})\mathbb{I} + \mathbf{d}[\mathbf{p},\Delta(t)]\cdot\boldsymbol{\sigma}, \tag{2}$$

where $\mathbf{p} = (p_x, p_y)$ is the two-dimensional momentum and $\boldsymbol{\sigma} = (\sigma_x, \sigma_y, \sigma_z)$ are the Pauli matrices, and $\Delta(t)$ is a gap parameter that varies as a function of time. When $\mathbf{d}[\mathbf{p},\Delta(t)]$ changes rapidly as in a quantum quench, the response depends intimately on the evolution of the wave function.

Before discussing the lattice setup, we first analyze a simple example that captures the essential physics—a quenched, single-cone, low-energy Haldane-type model—obeying Eq. (2) with

$$\epsilon_0(\mathbf{p}) = 0, \qquad \mathbf{d}[\mathbf{p},\Delta(t)] = (p_x, p_y, \Delta\Theta(-t)), \tag{3}$$

where $\Theta(t)$ is the Heaviside function. This captures the essential physics of the usual two-cone Haldane model up to a factor of 2, hence, the name. For $t < 0$, we begin in the many-body ground state $|\Psi_0\rangle$ at half-filling. For $t > 0$, the system coherently evolves with $|\Psi_1(t)\rangle = e^{-iHt}|\Psi_0\rangle = \prod_{\mathbf{p}}|\psi_1(\mathbf{p})\rangle$, where the single particle wave functions $|\psi_1(\mathbf{p})\rangle = e^{-ih(\mathbf{p},0)t}|\psi_0(\mathbf{p})\rangle$. For this half-filled band, the Chern number (defined by $\mathcal{C} = \int [d^2p/(2\pi)^2]\hat{\mathbf{z}}\cdot\nabla_{\mathbf{p}}\times\langle\psi_0(\mathbf{p})|i\nabla_{\mathbf{p}}|\psi_0(\mathbf{p})\rangle$) is $1/2$ per flavor. In equilibrium, this manifests as a $\sigma_{xy} = \mathcal{C}e^2/h$ bulk Hall conductivity, but as we show, the out-of-equilibrium current response becomes decoupled from the Chern number despite the fact that unitary evolution preserves $\mathcal{C}$ [17,21].

To extract the response properties of $|\Psi_1(t)\rangle$, we consider the following pulse-type protocol (see Fig. 1) where (i) at $t = t_1$ a short pulse $[E_x(t) = A_x\delta(t - t_1)]$ is applied to the system so that $\mathbf{p} \to \mathbf{p} - e\mathbf{A}$ [i.e., the Hamiltonian in Eq. (3) changes $\mathbf{d}(\mathbf{p},0) \to \mathbf{d}(\mathbf{p} - e\mathbf{A},0)$], (ii) and the Hall current, $\mathbf{J}_{\rm Hall}$, that develops is measured at $t = t_2$. Here, $t_1, t_2 > 0$ occur after the quench leading to a final state $|\Psi_2(t_2)\rangle = \prod_{\mathbf{p}}|\psi_2(\mathbf{p})\rangle$, with $|\psi_2(\mathbf{p})\rangle = e^{-i(t_2-t_1)h(\mathbf{p}-e\mathbf{A},0)}|\psi_1(\mathbf{p},t_1)\rangle$. In the following, we have set speed of light to unity.

The current response can be obtained via $\mathbf{J} = \langle\Psi|\hat{j}|\Psi\rangle$, where $\hat{j} = \partial H/\partial\mathbf{A}$. Using $|\Psi\rangle = |\Psi_2(t_2)\rangle$ along with Eq. (3) and extracting the component of $\mathbf{J}$ transverse to the applied field $\mathbf{E}$, we obtain $\mathbf{J}_{\rm Hall}$ as shown in Fig. 1(e). Here, $\mathbf{J}_{\rm Hall}$ was obtained via numerical integration with a

prequench $|\Psi_0\rangle$ where the entire valence band was filled. A full discussion of $\mathbf{J}$ is contained in the Supplemental Material [25]. Because of the collective action of all electrons in the valence band, $\mathbf{J}_{\mathrm{Hall}}$ does not have an apparent oscillatory structure in Fig. 1(e).

Strikingly, $\mathbf{J}_{\mathrm{Hall}}$ in Fig. 1(e) grows from zero (when the pulse is first applied at t_1) and saturates at long times to a nonvanishing value, $\mathbf{J}_{\mathrm{Hall}}(t_1, t_2 \to \infty) = \mathbf{J}^{\infty}_{\mathrm{Hall}}(t_1)$ as seen in Fig. 1(e). As we argue below, this behavior is generic for OES. The nonzero $\mathbf{J}^{\infty}_{\mathrm{Hall}}(t_1)$ is unconventional and arises from the near-lock-step Larmor precession of the pseudospinors $|\psi_1(\mathbf{p})\rangle$ that form the full many-body OES $|\Psi_1\rangle$.

We can understand this geometrically by considering Larmor precession of the pseudospins on the Bloch sphere. Even though we are interested in quenches defined in Eq. (3), the following geometric analysis is general and applies to two-band models. Mapping each spinor onto the Bloch sphere via $\hat{\mathbf{n}} = \langle\psi_1(\mathbf{p})|\boldsymbol{\sigma}|\psi_1(\mathbf{p})\rangle$, we can describe the Larmor precession of the spinors via the equations of motion

$$\partial_t \hat{\mathbf{n}} = 2\mathbf{d}(\mathbf{p}, 0) \times \hat{\mathbf{n}}, \qquad \hat{\mathbf{n}}(t = 0) = -\hat{\mathbf{d}}(\mathbf{p}, \Delta). \quad (4)$$

To understand why this implies a remnant Hall current, consider a ring of momenta with $|\mathbf{p}| = p$ held constant. With Larmor precession for $t > 0$, they will oscillate around a point on the equator, see Figs. 2(a) and 2(d). At time $t = t_1$ we apply a pulse. As shown by the red arrow in Fig. 2(b), the pulse has the effect of shifting the center of rotation for Larmor precession $\mathbf{d}(\mathbf{p}, 0) \to \mathbf{d}(\mathbf{p} - e\mathbf{A}, 0)$. As a result, at long times, the shift in average $\hat{\mathbf{n}}$ persists [see Figs. 2(b), 2(c), and 2(e)]. Since $\hat{\mathbf{n}}$ directly corresponds to current flow direction in Eq. (3), a remnant Hall current develops.

The long-time average of $\hat{\mathbf{n}}$ is just its projection at time t_1 along the new precession direction $\mathbf{d}(\mathbf{p} - e\mathbf{A}, 0)$ yielding

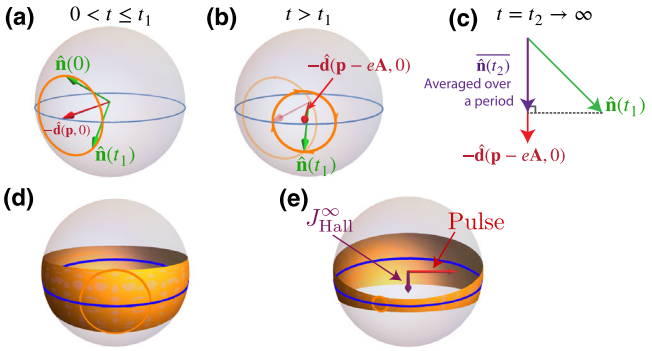

FIG. 2. (a) After quench, the state $\hat{\mathbf{n}}$ Larmor precesses on the Bloch sphere. (b) After the pulse, the center of Larmor precession shifts due to the momentum boost $e\mathbf{A}$. (c) For long times, the shift in the state's average over a Larmor period, $\overline{\hat{\mathbf{n}}(t_2)}$, persists leading to a current at $t_2 \to \infty$. (d) For the Haldane model, Eq. (3), the orange manifold represents the combined Larmor orbits of states with the same $|\mathbf{p}|$. (e) After the pulse, the manifold of Larmor orbits changes to give a perpendicular shift in the average $\overline{\hat{\mathbf{n}}(t_2)}$ resulting in $J^{\infty}_{\mathrm{Hall}}$.

$[\hat{\mathbf{n}}(t_1) \cdot \hat{\mathbf{d}}(\mathbf{p} - e\mathbf{A}, 0)]\hat{\mathbf{d}}(\mathbf{p} - e\mathbf{A}, 0)$. Writing the current operator as $\hat{j}_\mu = -e\partial_{p_\mu} h(\mathbf{p} - e\mathbf{A}, 0) = -e\partial_{p_\mu}\mathbf{d}(\mathbf{p} - e\mathbf{A}, 0) \cdot \boldsymbol{\sigma}$, we obtain the current from the projection of the average $\hat{\mathbf{n}}$ along $\partial_{p_\mu}\mathbf{d}(\mathbf{p} - e\mathbf{A}, 0)$. As a result, we find the long-time current for a state $\mathbf{p}$ as

$$j^{\infty}_{\mu}(\mathbf{p}, t_1) = -e[\hat{\mathbf{n}}(\mathbf{p}, t_1) \cdot \hat{\mathbf{d}}(\mathbf{p} - e\mathbf{A}, 0)]\partial_{p_\mu} d(\mathbf{p} - e\mathbf{A}, 0). \quad (5)$$

The expression in Eq. (5) is independent of a specific two-band model [26].

We now consider the quench specified in Eq. (3) so that $\hat{\mathbf{n}}(t_1) = \langle\psi_1|\boldsymbol{\sigma}|\psi_1\rangle$ reads as $\hat{\mathbf{n}}(t_1) = -\mathbf{p}\sin\theta_{\mathbf{p}} + (\cos 2pt_1\hat{\mathbf{z}} - \sin 2pt_1\hat{\mathbf{z}} \times \hat{\mathbf{p}})\cos\theta_{\mathbf{p}}$ [using $|\psi_1(\mathbf{p})\rangle$ derived earlier]. Integrating over all $\mathbf{p}$ (for a filled band prior to quench), we obtain a total current

$$J^{\infty}_{\mu}(t_1) = -e\int \frac{d^2p}{(2\pi\hbar)^2}\frac{\hat{\mathbf{n}}(t_1)\cdot(\mathbf{p} - e\mathbf{A})}{|\mathbf{p} - e\mathbf{A}|}\partial_{p_\mu}|\mathbf{p} - e\mathbf{A}|. \quad (6)$$

While this quantity can be fully evaluated (see Supplemental Material [25] for discussion), for brevity and to capture the essential physics, we expand Eq. (6) in $\mathbf{A}$. Discarding terms that integrate to zero, we arrive at Eq. (1) with $\Xi^{\infty}_{\mathrm{Hall}}(t_1) = -(e^2/2h)(\Delta/\hbar)\int_0^{\pi/2} dz e^{-2(t_1|\Delta|/\hbar)\sin z}$.

Even though $|\psi_1(\mathbf{p})\rangle$ with similar energies precess with frequencies that are close to each other, over long times t_1, small differences in their precession frequency allow their Larmor orbits to slowly drift out of phase, degrading $\mathbf{J}^{\infty}_{\mathrm{Hall}}(t_1)$. Analyzing $J^{\infty}_{\mathrm{Hall}}(t_1)$ for large t_1, we obtain

$$\mathbf{J}^{\infty}_{\mathrm{Hall}}(t_1) = -\mathrm{sgn}(\Delta)\frac{e^2}{4h}\frac{A_x}{t_1} + O(t_1^{-2}), \quad (7)$$

which shows that, the longer we wait after the quench to pulse the system, the smaller $\mathbf{J}^{\infty}_{\mathrm{Hall}}(t_1)$, as evidenced in the diminishing $\mathbf{J}_{\mathrm{Hall}}$ current profiles shown in Fig. 1(e). This aging behavior is a characteristic of the different energies of the pseudospinors that form prequench $|\Psi_0\rangle$.

Persistent $\mathbf{J}^{\infty}_{\mathrm{Hall}}$ does not occur in equilibrium systems; in fact, it is disallowed since dc conductivity is finite even without disorder. To see this, consider the response in equilibrium captured by $j_y(t) = \int \sigma_{yx}(t - t')E_x(t')dt'$. For a pulse $E_x(t) = A_x\delta(t)$, we have $j_y(t) = \sigma_{yx}(t)A_x$. Thus, $\sigma^{\mathrm{dc}}_{yx} = (1/A_x)\int j_y(t)dt$. As a result, for $\sigma^{\mathrm{dc}}_{yx}$ that is finite (e.g., the anomalous and conventional Hall effect, the quantum Hall effect), then $j_y(t) \to 0$ as $t \to \infty$ due to integrability.

Relaxation can be included in Eq. (4) in the form of a T_1 and T_2 time [27]. Oscillatory terms describing the Larmor precession are all that are affected by T_2, so if we isolate the nonoscillatory term which gives rise to Eq. (5), we find that only energy relaxation in the form of T_1 time affects

the result. In fact, at long times, $j_\mu(\mathbf{p}, t_2, t_1) = j^\infty_\mu(\mathbf{p}, t_1)e^{-t_2/T_1(p)}$. We expect relaxation processes to occur with a probability roughly determined by Fermi's golden rule such that $1/T_1(p) \sim \gamma\rho[\epsilon(p)]$ where $\rho(\epsilon)$ is the density of states and γ describes the relaxation. In the above model [Eq. (3)], this leads to a suppression as $1/t_2^2$ at long times for $\mathbf{J}_{\mathrm{Hall}}$ (see Supplemental Material [25]).

OES Hall currents in Eq. (1) depend intimately on the underlying symmetries of the Hamiltonian, h, in Eq. (2). In particular, we find $\Xi^\infty_{\mathrm{Hall}}$ depends on the absence of either mirror, $M_y^{-1}h(p_x, p_y)M_y = h(p_x, -p_y)$, or time-reversal, $T^{-1}h(-\mathbf{p})T = h(\mathbf{p})$, symmetry. To expose this, we analyze the contribution of $\mathbf{p}$ states to the persistent response in Eq. (5). Expanding in the pulse strength $\mathbf{A}$, we obtain $j^\infty_\mu(\mathbf{p}, t_1) \approx \chi^\infty_{\mu\nu}(\mathbf{p}, t_1)A_\nu$. Indeed, $\Xi^\infty_{\mathrm{Hall}} = \int d\mathbf{p}\chi^\infty_{\mathrm{Hall}}(\mathbf{p})$, where $\chi^\infty_{\mathrm{Hall}} = \frac{1}{2}(\chi^\infty_{yx} - \chi^\infty_{xy})$. Writing $\mathbf{d}_0 = \mathbf{d}(\mathbf{p}, 0)$ yields $\chi^\infty_{\mathrm{Hall}} = \chi^\infty_M + \chi^\infty_T$, where $\chi^\infty_M = e^2\partial_{[p_y}d_0\partial_{p_x]}\hat{\mathbf{d}}_0 \cdot \hat{\mathbf{d}}\cos 2d_0t_1$, and $\chi^\infty_T = -e^2\partial_{[p_y}d_0\partial_{p_x]}\hat{\mathbf{d}}_0 \cdot \hat{\mathbf{d}}_0 \times \hat{\mathbf{d}}\sin 2d_0t_1$. Here, the brackets $\partial_{[p_y}\cdots\partial_{p_x]}$ denote antisymmetrization, and M and T subscripts denote contributions controlled by M_y and T. Importantly, if h possesses M_y symmetry, then $\chi^\infty_M(p_x, p_y) = -\chi^\infty_M(p_x, -p_y)$. On the other hand, if h possesses T symmetry, then $\chi^\infty_T(\mathbf{p}) = -\chi^\infty_T(-\mathbf{p})$ (see Supplemental Material [25]). As a result, when h satisfies both M_y and T symmetries (before and after quench), opposing momentum states will give contributions of opposite sign, and $\Xi^\infty_{\mathrm{Hall}} = \int d\mathbf{p}\chi^\infty_{\mathrm{Hall}}(\mathbf{p}) = 0$. Hence, finite $\Xi^\infty_{\mathrm{Hall}}$ arises from breaking of either M_y or T symmetry before or after the quench [28] in contrast to the symmetry requirements for Hall currents in equilibrium linear response [29].

While the OES Hall response is disconnected from the Chern number, $\mathcal{C}$, $\Xi^\infty_{\mathrm{Hall}}$ can still be expressed in terms of bulk band properties. In particular, for M_y symmetric Hamiltonians with a filled band prior to quench, we find an equivalent Thouless-Kohomoto-Nightingale-den Nijs (TKNN)-like formula

$$\Xi^\infty_{\mathrm{Hall}} = -e^2\int \frac{d^2p}{(2\pi)^2}\partial_{t_1}\Omega_{p_yp_x}\log d(\mathbf{p}, 0), \qquad (8)$$

where $\Omega_{p_yp_x} = \frac{1}{2}\hat{\mathbf{n}}(t_1) \cdot [\partial_{p_y}\hat{\mathbf{n}}(t_1) \times \partial_{p_x}\hat{\mathbf{n}}(t_1)]$ is the Berry curvature of the evolved $\mathbf{p}$ state evaluated at pulse time t_1. While arising from Berry curvature, we note that it is manifestly distinct from $\mathcal{C}$ and is not quantized.

Finally, we examine other quench protocols for Eq. (2). As we will see, these yield similar responses to the Haldane protocol examined above. One interesting example is a Rashba type protocol where

$$\epsilon_0(\mathbf{p}) = \frac{p^2}{2m}, \quad \mathbf{d}(\mathbf{p}, \Delta) = (-v_{\mathrm{F}}p_y, v_{\mathrm{F}}p_x, \Delta\Theta(-t)), \qquad (9)$$

and chemical potential $\mu = 0$. As shown in Figs. 3(a) and 3(b), the Rashba protocol also yields a Hall current that persists at long times. Interestingly, the Hall current in Fig. 3(a) exhibits an oscillatory behavior which arises from the momentum cutoff of Eq. (9) at $p_F = v_F[2m(mv_F^2 + \sqrt{m^2v_F^4 + \Delta^2})]^{1/2}$; this contrasts with the smooth behavior of Fig. 1(e), which had no momentum cutoff.

For $t_2 \to \infty$, the Hall current response levels out [Figs. 3(a) and 3(b)]. Indeed, its persistent response, $\mathbf{J}^\infty_{\mathrm{Hall}}$, matches the Haldane protocol closely [see Fig. 3(a)], except in one important way. In the Rashba protocol, it takes a finite t_1 to "turn on" $\mathbf{J}^\infty_{\mathrm{Hall}}$: magnitude $\mathbf{J}^\infty_{\mathrm{Hall}}$ increases from zero at small t_1, and decreases at long t_1. In contrast, the Haldane protocol has maximal $\mathbf{J}^\infty_{\mathrm{Hall}}$ at $t_1 \to 0^+$. This difference arises due to the momentum cutoff which does not appear in the low-energy model of Eq. (3) where there exist states on the Bloch sphere that have already performed multiple Larmor orbits even for an infinitesimal t_1, yielding a large $\mathbf{J}^\infty_{\mathrm{Hall}}$.

Quench type protocols exhibiting $\mathbf{J}^\infty_{\mathrm{Hall}}$ can also be realized in lattice models. In these, the bands are finite as opposed to the continuum bands discussed above. We illustrate such a protocol for a "half-Bernevig-Hughes-Zhang" type model in a square lattice [30], wherein Eq. (2) takes $\epsilon_0(\mathbf{p}) = 0$ and $\mathbf{d}[\mathbf{p}, M(t)] = (\hbar v_{\mathrm{F}}/a)[\sin(ap_x/\hbar), \sin(ap_y/\hbar), M(t) + 2 - \cos(ap_x/\hbar) - \cos(ap_y/\hbar)]$. Here, $M(t < 0) = M$ and $M(t > 0) = M'$ represents the quench, and a is the lattice constant. In the ground state, this model has different topological phases represented by M [31]. Picking M, M' values allows us to quench within and between the trivial and topological phases, yielding a persistent Hall current as well [Fig. 3(c)]. As in the case of the Rashba Hamiltonian, there is turn-on behavior with a time scale corresponding to the momentum cutoff provided by a^{-1}.

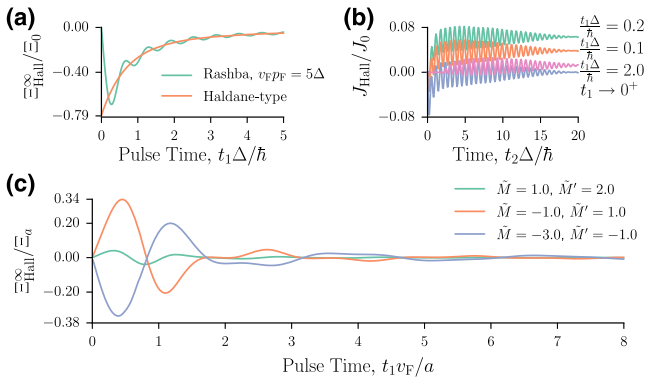

FIG. 3. Other models exhibiting a remnant Hall current from OES. (a) The long-time remnant $\Xi^\infty_{\mathrm{Hall}}$ dies off as a function of pulse time t_1 for Haldane and Rashba models. The Fermi momentum cutoff in the Rashba model causes oscillations and $\Xi_{\mathrm{Hall}} \to 0$ as $t_1 \to 0$. (b) For the Rashba model, the current evolves in an oscillatory way due to the cutoff p_{F}. (c) Remnant $\Xi^\infty_{\mathrm{Hall}}$ in the half-BHZ model (see text) sees similar oscillations due to the cutoff provided by the square lattice. Interestingly, $\Xi^\infty_{\mathrm{Hall}} \neq 0$, regardless of the phase we begin or end in. For the Rashba model, we used $eA_x = 0.1\Delta/v_F$ and $v_{\mathrm{F}}p_F = 5\Delta$. In the above, characteristic $J_0 = (e^2/h)(\Delta^2/e\hbar v_F)$, $\Xi_0 = (e^2/h)(\Delta/\hbar)$, $\Xi_a = (e^2/h)(v_F/a)$, and $\tilde{M} = M(a/\hbar v_F)$.

The general framework, as well as the specific model realizations, presented here demonstrate that OES prepared via a quench can manifest Hall currents that persist long after the application of an excitation pulse. Strikingly, they occur under different symmetry requirements than that found in equilibrium systems and can arise even when the instantaneous Hamiltonian is TRS preserving. The experimental conditions necessary for probing OES are readily available in current cold atom setups [32]. In particular, the remnant, quench-induced Hall currents described can be measured via time of flight and provides a new diagnostic of coherent wave function dynamics. The Hall response of OES depends intimately on the entire history of wave function evolution, unlike that found in equilibrium. This opens a new vista of unconventional phenomena that can be prepared and probed in OES.

We thank Mehrtash Babadi, Eugene Demler, and Ian Spielman for helpful discussions. We thank the Air Force Office for Scientific Research (J. W.) and the Burke fellowship at the Walter Burke Institute of Theoretical Physics, Caltech (J. C. W. S.) for support. G. R. is grateful for support through the Institute of Quantum Information and Matter (IQIM), an National Science Foundation frontier center, supported by the Gordon and Betty Moore Foundation as well as the Packard Foundation and for the hospitality of the Aspen Center for Physics, where part of the work was performed.

Note added.—Recently, we became aware of the complementary work of Hu, Zoller, and Budich [33] on out-of-equilibrium Hall responses. They include breaking of translational invariance (by a trap, for instance) and find little effect to the out-of-equilibrium Hall response.

*jwilson@caltech.edu
†Present address: Division of Physics and Applied Physics, Nanyang Technological University and Institute of High Performance Computing Singapore.
justinsong@ntu.edu.sg

[1] K. Von Klitzing, The quantized Hall effect, Rev. Mod. Phys. **58**, 519 (1986).
[2] N. Nagaosa, J. Sinova, S. Onoda, A. H. MacDonald, and N. P. Ong, Anomalous Hall effect, Rev. Mod. Phys. **82**, 1539 (2010).
[3] H. L. Stormer, D. C. Tsui, and A. C. Gossard, The fractional quantum Hall effect, Rev. Mod. Phys. **71**, S298 (1999).
[4] K. V. Klitzing, G. Dorda, and M. Pepper, New Method for High-Accuracy Determination of the Fine-Structure Constant Based on Quantized Hall Resistance, Phys. Rev. Lett. **45**, 494 (1980).
[5] Y.-J. Lin, K. Jiménez-García, and I. B. Spielman, Spin–orbit-coupled Bose–Einstein condensates, Nature (London) **471**, 83 (2011).
[6] I. Bloch, J. Dalibard, and S. Nascimbène, Quantum simulations with ultracold quantum gases, Nat. Phys. **8**, 267 (2012).
[7] S. Will, D. Iyer, and M. Rigol, Observation of coherent quench dynamics in a metallic many-body state of fermions, Nat. Commun. **6**, 6009 (2015).
[8] B. K. Stuhl, H. I. Lu, L. M. Aycock, D. Genkina, and I. B. Spielman, Visualizing edge states with an atomic Bose gas in the quantum Hall regime, Science **349**, 1514 (2015).
[9] G. Jotzu, M. Messer, R. Desbuquois, M. Lebrat, T. Uehlinger, D. Greif, and T. Esslinger, Experimental realization of the topological Haldane model with ultracold fermions, Nature (London) **515**, 237 (2014).
[10] M. Atala, M. Aidelsburger, J. T. Barreiro, D. Abanin, T. Kitagawa, E. Demler, and I. Bloch, Direct measurement of the Zak phase in topological Bloch bands, Nat. Phys. **9**, 795 (2013).
[11] M. Killi, S. Trotzky, and A. Paramekanti, Anisotropic quantum quench in the presence of frustration or background gauge fields: A probe of bulk currents and topological chiral edge modes, Phys. Rev. A **86**, 063632 (2012).
[12] P. Hauke, M. Lewenstein, and A. Eckardt, Tomography of Band Insulators from Quench Dynamics, Phys. Rev. Lett. **113**, 045303 (2014).
[13] A. G. Grushin, S. Roy, and M. Haque, Response of fermions in Chern bands to spatially local quenches, J. Stat. Mech.: Theory Exp. **2016**, 083103 (2016).
[14] M. Greiner, O. Mandel, T. W. Hänsch, and I. Bloch, Collapse and revival of the matter wave field of a Bose-Einstein condensate, Nature (London) **419**, 51 (2002).
[15] T. Oka and H. Aoki, Photovoltaic Hall effect in graphene, Phys. Rev. B **79**, 081406(R) (2009).
[16] T. Kitagawa, T. Oka, A. Brataas, L. Fu, and E. Demler, Transport properties of nonequilibrium systems under the application of light: Photoinduced quantum Hall insulators without Landau levels, Phys. Rev. B **84**, 235108 (2011).
[17] L. D'Alessio and M. Rigol, Dynamical preparation of Floquet Chern insulators, Nat. Commun. **6**, 8336 (2015).
[18] M. S. Rudner, N. H. Lindner, E. Berg, and M. Levin, Anomalous Edge States and the Bulk-Edge Correspondence for Periodically Driven Two-Dimensional Systems, Phys. Rev. X **3**, 031005 (2013).
[19] L. E F Foa Torres, P. M. Perez-Piskunow, C. A. Balseiro, and G. Usaj, Multiterminal Conductance of a Floquet Topological Insulator, Phys. Rev. Lett. **113**, 266801 (2014).
[20] J. C. Budich and M. Heyl, Dynamical topological order parameters far from equilibrium, Phys. Rev. B **93**, 085416 (2016).
[21] M. D. Caio, N. R. Cooper, and M. J. Bhaseen, Quantum Quenches in Chern Insulators, Phys. Rev. Lett. **115**, 236403 (2015).
[22] H. Dehghani, T. Oka, and A. Mitra, Out-of-equilibrium electrons and the Hall conductance of a Floquet topological insulator, Phys. Rev. B **91**, 155422 (2015).
[23] M. Stark and M. Kollar, Kinetic description of thermalization dynamics in weakly interacting quantum systems, arXiv:1308.1610.
[24] B. Bertini and M. Fagotti, Pre-relaxation in weakly interacting models, J. Stat. Mech. (2015) P07012.
[25] See Supplemental Material at http://link.aps.org/supplemental/10.1103/PhysRevLett.117.235302 for calculational details.

[26] A two-band model neglecting current contributions from $\epsilon_0(\mathbf{p})$; however, those contributions do not have a Hall response.

[27] D. Budker, D. F. Kimball, and D. P. DeMille, *Atomic Physics: An Exploration through Problems and Solutions* (Oxford University Press, New York, 2008).

[28] Indeed, h in Eq. (3) possesses M_y symmetry (antiunitary symmetry), but $h(t<0)$ breaks T symmetry resulting in the observed Hall current.

[29] I. Sodemann and L. Fu, Quantum Nonlinear Hall Effect Induced by Berry Curvature Dipole in Time-Reversal Invariant Materials, Phys. Rev. Lett. **115**, 216806 (2015).

[30] B. A. Bernevig and T. L. Hughes, *Topological Insulators and Topological Superconductors* (Princeton University Press, 2013) p. 264.

[31] $M>0$ and $M<-4$ are trivial with equilibrium $\sigma_{xy}=0$, $-2<M<0$ is a topological insulator with equilibrium $\sigma_{xy}=-1$, and $-4<M<-2$ is also a topological insulator with equilibrium $\sigma_{xy}=+1$.

[32] D. M. Stamper-Kurn and M. Ueda, Spinor Bose gases: Symmetries, magnetism, and quantum dynamics, Rev. Mod. Phys. **85**, 1191 (2013).

[33] Y. Hu, P. Zoller, and J. C. Budich, Dynamical Buildup of a Quantized Hall Response from Nontopological States, Phys. Rev. Lett. **117**, 126803 (2016).